Atmos. Meas. Tech., 18, 3945–3958, 2025
https://doi.org/10.5194/amt-18-3945-2025

Atmospheric Measurement Techniques
Open Access
EGU

The coupling of a high-efficiency aerosol collector with electrospray ionisation–Orbitrap mass spectrometry as a novel tool for real-time chemical characterisation of fine and ultrafine particles

Yik-Sze Lau, Zoran Ristovski, and Branka Miljevic

International Laboratory for Air Quality and Health, School of Earth and Atmospheric Sciences, Queensland University of Technology, Brisbane, Australia

Correspondence: Branka Miljevic (b.miljevic@qut.edu.au)

Received: 25 November 2024 – Discussion started: 3 January 2025
Revised: 8 May 2025 – Accepted: 8 May 2025 – Published: 25 August 2025

Abstract. The chemical properties of aerosols in the atmosphere significantly influence their impact on the global climate forcing and human health. However, a real-time molecular-level characterisation of aerosols remains challenging due to the complex nature of their chemical composition. The current study constructed an instrumental system for the real-time chemical characterisation of aerosol particles. The proposed setup consists of a custom-built high-efficiency aerosol collector (HEAC) used to collect aerosol samples into a working fluid and an electrospray ionisation (ESI) Orbitrap mass spectrometer (MS) for the subsequent chemical analysis of the liquid sample. The HEAC/ESI-Orbitrap-MS was calibrated against six chemical compounds – vanillic acid (VA), adonitol, erythritol, tricarballylic acid (TCA), sucrose, and trehalose – to investigate the system's sensitivity and limit of detection (LOD). Results showed that the coupled system has high sensitivities to the tested chemical compounds and a similar, if not better, LOD than other related instrumental techniques. The 3σ LOD of the tested compounds ranged from $1.1 \pm 0.14\,\mathrm{ng\,m^{-3}}$ (erythritol) to $65 \pm 7.4\,\mathrm{ng\,m^{-3}}$ (TCA). The capability of the HEAC/ESI-Orbitrap-MS system to identify the chemical composition of organic aerosols (OAs) was also examined. Sample OA was generated by α-pinene ozonolysis, and the chemical characterisation results were compared to similar studies. Our data showed that the HEAC/ESI-Orbitrap-MS system can identify most of the α-pinene ozonolysis products reported in the literature, including cis-pinonic acid, pinalic acid, and 3-methyl-1,2,3-butanetricarboxylic acid (MBTCA). Monomeric and dimeric reaction products were accurately identified in the mass spectra, even at a total OA mass concentration $< 2\,\mathrm{\mu g\,m^{-3}}$. The present study showed that the HEAC/ESI-Orbitrap-MS system is a robust technique for the real-time chemical characterisation of OA particles under atmospherically relevant conditions.

1 Introduction

Aerosols are small solid or liquid particles suspended in the atmosphere. They can be categorised by aerodynamic diameter into coarse ($d_a > 2.5\,\mu m$), fine ($0.1\,\mu m < d_a < 2.5\,\mu m$), and ultrafine ($d_a < 0.1\,\mu m$) particles (Kulkarni et al., 2011). Chemically, aerosols rich in inorganic materials like sulfates and sea salt are called inorganic aerosols, while those dominated by organic matter are called organic aerosols (OAs). Previous studies have shown that OA constitutes 20 %–90 % of the fine-particle mass in tropospheric aerosols (Kanakidou et al., 2005; Jimenez et al., 2009). Aerosols affect air quality and human health significantly (Pöschl, 2005; Huang et al., 2014), leading to extensive studies on their physical and chemical properties (Tao et al., 2017; Quinn et al., 2015; Fan et al., 2016; Shrivastava et al., 2017). Fine and ultrafine aerosols are particularly important due to their complex environmental reactions and deep penetration into the respiratory system (Shiraiwa et al., 2017; Kwon et al., 2020; Bates et al., 2019). Aerosols also impact global climate directly by affecting the radiative budget through the absorption and reflection of radiation and indirectly by acting as cloud condensation nuclei (CCN) (Mahowald et al., 2011; Mcneill, 2017). Changes in aerosol chemical composition can alter their op-

tical properties and CCN formation abilities, affecting their radiative forcing. Therefore, understanding aerosol chemical composition is crucial for assessing their environmental, health, and climate impacts.

Traditionally, molecular-level characterisations of aerosols were typically done through offline analyses. Aerosol samples were collected on filters, followed by sample extractions, derivatisation, and instrumental analyses (Fleming et al., 2020; Sun et al., 2016). The most utilised techniques for identifying and quantifying chemical species in aerosols are gas chromatography–mass spectrometry (GC/MS) and liquid chromatography–mass spectrometry (LC/MS) (Kautzman et al., 2010; Budisulistiorini et al., 2015). Offline analyses are advantageous due to well-developed protocols and extensive databases, facilitating the chemical characterisation of aerosol samples. Various techniques can be used to obtain detailed information on the chemical compounds under study. For example, ion mobility spectrometry–mass spectrometry (IMS/MS) can be used to differentiate between isomers of compounds with the same chemical formula (Krechmer et al., 2016). However, they lack a time resolution, making it challenging to track changes in chemical composition over time. Additionally, offline methods require several sample preparation steps, which can introduce errors and alter the sample composition (Miljevic et al., 2014). Also, using filters for sample collection may result in positive sampling artefacts as they may adsorb a portion of the semi-volatile compounds in the sampled air (Kirchstetter et al., 2001).

As the evolution of the aerosol's chemical composition is critical for understanding its chemistry in different processes, online techniques have been developed to tackle this challenge. The aerosol mass spectrometer (AMS) is widely used for real-time bulk chemical composition analysis, providing crucial information on the chemical and physical properties of aerosols. However, the AMS uses a hard ionisation source (electron impact ionisation), resulting in mass spectra with mostly fragmented ion peaks, which are grouped into organics and several inorganic ions such as sulfate, nitrate, chloride, and ammonium (Canagaratna et al., 2007). Recently, a CHARON (CHemical analysis of AeRosol ONline) inlet coupled with a proton transfer reaction time-of-flight mass spectrometer (PTR-TOF-MS) and an extractive electrospray ionisation- (EESI) TOF-MS were developed for the real-time, direct molecular-level analysis of aerosol chemical composition in ambient air (Lopez-Hilfiker et al., 2019; Piel et al., 2019). However, these instruments have drawbacks. The PTR-TOF-MS can only detect compounds with proton affinities higher than that of H_2O, and switching ion sources to detect a wider array of compounds may require changes in instrumental configurations. Additionally, although the TOF mass analyser used in both instruments can provide sufficient resolution for compounds with low molecular weight, it cannot unambiguously separate isobaric compounds in complex mixtures, making post-experiment data analysis challenging.

Several studies have employed a different approach to obtain a time-resolved chemical composition profile of fine particles using a particle-into-liquid sampler (PILS) coupled with various mass spectrometry systems for online chemical characterisation of aerosols. For example, Zhang et al. (2016) coupled the PILS with the ultra performance liquid chromatography–ESI quadrupole time-of-flight mass spectrometer (UPLC/ESI-Q-TOF-MS) to analyse atmospheric aerosol samples, demonstrating sufficient sensitivity and detection limits for single compounds at concentrations of micrograms to nanograms per cubic metre. Their system was used to chemically characterise the reactive uptake products of isoprene epoxydiols on acidic ammonium sulfate aerosols. Saarnio et al. (2013) combined the PILS with high-performance anion exchange chromatography (HPAEC)-MS to measure levoglucosan in ambient aerosols, while Parshintsev et al. (2010) used the PILS with solid-phase extraction (SPE)-LC–ion trap MS to investigate organic acids in aerosols. While the separation techniques employed by the above studies benefit the chemical characterisation of the OA samples, the downside is that they are only partially real time. This is because PILS-collected samples were either stored in vials or the LC system's sample injection loop before MS analysis, with the time resolution depending on the collection or injection frequency. For example, the time resolutions for the PILS-UPLC/ESI-Q-TOFMS and the PILS-HPAEC-MS were 5 and 8 min, respectively. Additionally, improving the mass resolution of these MS systems could enhance the peak separation and identification of reaction products. Therefore, it is necessary to construct a new system that can provide real-time determination of aerosol chemical composition at atmospherically relevant mass loadings. Stockwell et al. (2018) have coupled the PILS with an ESI quadrupole MS (PILS/ESI-QMS) in a direct-infusion manner to obtain real-time information on reactive nitrogen species in aerosol samples. The proposed system in the current study has a similar configuration to the PILS/ESI-QMS, which consists of a custom-built aerosol collection system as described in Brown et al. (2019b) and is coupled to a high-mass-resolution mass spectrometer, namely the Orbitrap MS.

The high-efficiency aerosol collector (HEAC) achieves nearly 100 % collection efficiency for fine and ultrafine particles down to 30 nm (Brown et al., 2019b). The HEAC operates similarly to the particle-into-liquid sampler (PILS), using condensational growth of aerosol particles to enhance their collection efficiency. While the PILS uses a washed-wall collector, the HEAC employs a vortex collector – a cyclone with a standing liquid vortex on its wall during operation (Orsini et al., 2008). The Orbitrap MS used in the current study is a commercialised mass spectrometric technique that offers a high mass resolution. In recent years, several high-resolution mass spectrometric techniques have been commercialised, allowing researchers to obtain detailed molecular information with minimal peak overlap. One such technique is the Orbitrap mass analyser coupled with an ESI

source (Zubarev and Makarov, 2013). The ESI-Orbitrap-MS offers a mass resolution above 100 000, suitable for analysing complex mixtures containing numerous compounds, such as organic aerosol (OA) samples. Using an ESI source can also preserve the molecular identity of chemical compounds in the sample.

The objective of the current study was to assess the performance of the newly constructed HEAC/ESI-Orbitrap-MS system. The system's sensitivity and detection limits were assessed using various chemical compounds, and its capability of providing real-time chemical information on aerosol samples was evaluated by analysing the products of α-pinene ozonolysis.

2 Methodology

2.1 Coupling of HEAC and ESI-Orbitrap-MS

Detailed design and characterisation of the HEAC can be found elsewhere (Brown et al., 2019b). Briefly, the aerosol sample flows through the HEAC inlet at a typical rate of $16.7\,\mathrm{L\,min^{-1}}$, reaching a condensation growth chamber. Here, the aerosol encounters a parallel jet of steam, and the rapid cooling of the steam creates supersaturated conditions in the chamber. This causes the aerosol particles to grow into droplets of a few microns in size. These droplets were collected by the conical vortex collector at the chamber exit. When in operation, a vortex working fluid flows from the top to the bottom of the vortex collector and forms a thin film of liquid on the walls of the cyclone. Detailed operation principles of the vortex collector are available elsewhere (Brown et al., 2019b; Orsini et al., 2008). The working fluid flow rate out of the vortex collector was set to $1\,\mathrm{mL\,min^{-1}}$ during method development, consistently with previous applications (Brown et al., 2020, 2019a). The collected aerosol sample can be analysed instrumentally without further preparation.

The ESI-Orbitrap-MS (LTQ Orbitrap Elite, Thermo Fisher, USA) in this study is managed by the Central Analytical Research Facility (CARF) at the Queensland University of Technology (QUT). To connect the HEAC to the ESI source of the MS, the vortex collector outlet can be linked directly to the ESI sample inlet. However, the peristaltic pump (ISMATEC Reglo ICC 4 channel, Cole-Parmer, USA) controlling the HEAC's liquid flows does not generate enough pressure to deliver the sample through the ESI source's capillary nozzle. To address this, a high-pressure auxiliary pump (Dionex AXP, Thermo Fisher, USA) was used to draw some liquid from the vortex collector and inject it into the ESI source. Figure 1 shows a schematic diagram of the setup. Ethylene tetrafluoroethylene tubing (ETFE, $1/16''$ outer diameter, $0.04''$ inner diameter, IDEX Health and Science, USA) was used for the liquid flow lines upstream of the auxiliary pump. In contrast, polyether ether ketone tubing (PEEK, $1/16''$ outer diameter, $0.005''$ inner diameter, IDEX Health and Science, USA) was used to connect the auxiliary pump and the ESI source. The sample flow rate to the ESI source was set to $0.5\,\mathrm{mL\,min^{-1}}$. The ESI-Orbitrap-MS was run in negative-ion mode, with a spray voltage of $-3.5\,\mathrm{kV}$.

2.2 Characterisation of the HEAC/ESI-Orbitrap-MS system

The characterisation of the HEAC/ESI-Orbitrap-MS system is divided into two parts. The first part evaluates the system's sensitivity and detection limits for various chemical compounds under different conditions. The second part assesses the system's ability to analyse a complex organic aerosol sample generated from α-pinene ozonolysis.

2.2.1 Sensitivity and detection limit of the HEAC/ESI-Orbitrap-MS system

To characterise the sensitivities and detection limits of the HEAC/ESI-Orbitrap-MS system, the mass concentration of a chemical compound measured before entering the HEAC is compared with the compound's signal intensity as measured by the ESI-Orbitrap-MS. Figure S1 in the Supplement shows a schematic of the setup for single-compound characterisation. Briefly, each examined compound was dissolved in around 50 mL of Milli-Q water and nebulised by an atomiser (Collison 1-jet, CH Technologies, USA). All examined compounds except adonitol had a mass concentration of around $0.5\,\mathrm{g\,L^{-1}}$. The mass concentration of adonitol in the atomiser was around $3\,\mathrm{g\,L^{-1}}$. The nebulised sample was then pushed through a diffusion dryer filled with silica gel. The sample flow from the dryer was mixed with filtered air to provide a sufficient flow volume for the HEAC ($16.7\,\mathrm{L\,min^{-1}}$). Before entering the HEAC, the mass concentration of the diluted sample was measured by a scanning mobility particle sizer (SMPS) system (electrostatic classifier 3080 and condensation particle counter 3776, TSI Incorporated, USA, with a custom-built column). The mass concentration of the sample was calculated from the measured size distribution assuming that the particles are spherical and with the same density as their pure solid form.

To estimate the sensitivity of a particular chemical compound in the HEAC/ESI-Orbitrap-MS system, a calibration curve of mass concentration versus ESI-Orbitrap-MS signal is needed. The mass concentration entering the system was varied by adjusting the compressed air flow rate into the atomiser. For each concentration, the ESI-Orbitrap-MS signal was measured continuously for at least 5 min to obtain a steady average. The sample mass concentrations measured by the SMPS were also averaged. Sensitivity is determined by finding the slope of the best-fit line of the calibration curve. Details of the calculation can be found in the sensitivity and limit of detection (LOD) calculations section in the Supplement.

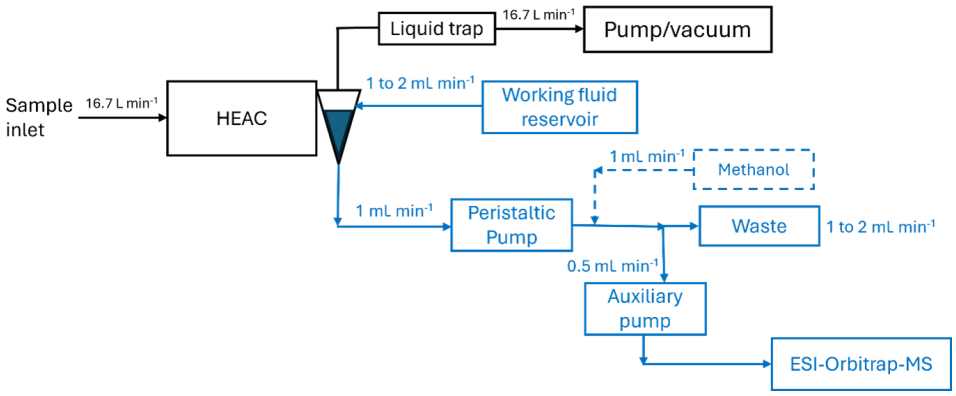

Figure 1. Schematic diagram of the HEAC/ESI-Orbitrap-MS system. Components in blue indicate liquid flow paths and flow rates. Dashed lines indicate the additional setup when using Milli-Q water as the working fluid.

Six chemical compounds – vanillic acid (VA), adonitol, erythritol, tricarballylic acid (TCA), sucrose, and trehalose – were used for sensitivity and limit of detection (LOD) experiments due to their varying water solubilities, volatilities, and relevance to atmospheric chemistry. Their physical properties are detailed in Table S1 in the Supplement. Milli-Q water was used as the working fluid for the sensitivity and LOD characterisation experiments. To assist in the ionisation of samples, methanol was added to the sample flow via a T junction before the auxiliary pump whenever Milli-Q water was used as the working fluid.

To account for variations in signal intensity from the ESI process, malic acid ($\sim 0.1\,\mu M$) was added to the vortex collector's working fluid. All ESI-Orbitrap-MS data in the sensitivity and LOD calculations were corrected based on the malic acid signal.

The study also examined the sensitivity and LOD of the HEAC/ESI-Orbitrap-MS using different working fluids as the ionisation efficiency and, thus, the sensitivity and LOD can be significantly affected by the choice of solvent. The solvents tested were Milli-Q (MQ) water, methanol, and acetonitrile (ACN), which are commonly used in ESI-MS. The experimental procedures remained consistent with the sensitivity and LOD characterisation experiments, except for the variation in the working fluid.

2.2.2 α-pinene ozonolysis experiment

To validate the HEAC/ESI-Orbitrap-MS system, α-pinene ozonolysis was conducted in a custom-built 5 L reaction bottle, and the particle-phase products were analysed by the system. Two types of α-pinene ozonolysis experiments were performed: fast injection and slow injection. The setups for both are shown in Fig. S1. In both experiments, α-pinene ozonolysis occurred in the reaction bottle. Ozone was generated by pushing $0.3\,L\,min^{-1}$ compressed air through an ozone generator (SOG-2, Analytik Jena US, USA), achieving a concentration of ~ 2 ppm in the bottle. For the fast injection, 20 µL of α-pinene was directly injected into the reaction bottle through a small hole in the cap, evaporating in less than 5 min. For the slow injection, 100 µL of α-pinene in a three-necked round bottom flask was placed before the reaction bottle, with ozone passing through it first. This setup slowed the evaporation rate of α-pinene, taking 15–20 min for complete evaporation.

After passing through the reaction bottle, the product mixture was pushed through a diffusional dryer containing charcoal (hereafter referred to as a charcoal filter) to remove the excess ozone and gas-phase products. Afterwards, the gas stream was mixed with a makeup flow of charcoal- and high-efficiency particulate air (HEPA)-filtered lab air to compensate for the sampling volume of the HEAC. For the experiment with fast α-pinene injection, the mixed sample flow was sampled by the custom-built SMPS for its size distribution before being analysed by the HEAC/ESI-Orbitrap-MS system. The mass concentration of particles was calculated from the measured size distribution assuming a particle density of $1.2\,g\,cm^{-3}$ (Shilling et al., 2009). For the experiment with slow α-pinene injection, after the sample was mixed with the make-up flow, the sample flow went through one of three scenarios before going into the HEAC: (1) passing through a HEPA filter, (2) passing through a charcoal filter, and (3) passing through no filter. This sequence was repeated four times, and the switching between each scenario was carried out manually by means of a three-way valve. The rotation of different scenarios aims to examine the system's response time and to determine whether the samples are all in the particle phase.

It should be noted that the α-pinene ozonolysis experiment carried out in the current study serves to assess the performance of the new HEAC/ESI-Orbitrap-MS system. Atmospheric relevance was not considered in the experimental design, and the results should not be used to compare directly with other studies under atmospherically relevant conditions.

2.3 Product identification in α-pinene ozonolysis experiments

A third-party software, MZmine (ver. 3.9) (Schmid et al., 2023), was used for product identification in α-pinene ozonolysis experiments. A detailed workflow and parameterisation of the software are outlined in the α-pinene ozonolysis product identification section in the Supplement. Briefly, the experiment's raw data file contains a time profile of mass spectra corresponding to the real-time measurement of samples collected by the HEAC at a time resolution of around 0.8 s. After the raw data were imported to Mzmine, "mass detection" was done to identify all of the ions present in every mass spectrum with signal intensities above certain thresholds (e.g. noise level and separations between ion signals). A mass list was generated for all mass spectra. A "feature detection" algorithm was then applied to the raw data to create the time series of all ions in the mass list that fulfil the criteria set in the algorithm (Pluskal et al., 2010; Myers et al., 2017). At the current threshold settings, 204 000 ions of different m/z were identified by the mass detection algorithm, and the time series of 20 004 ions were obtained from the feature detection function. These time series were then individually inspected. Ions were assigned as "product ions" if their signals increased when the HEAC was sampling from the reaction bottle.

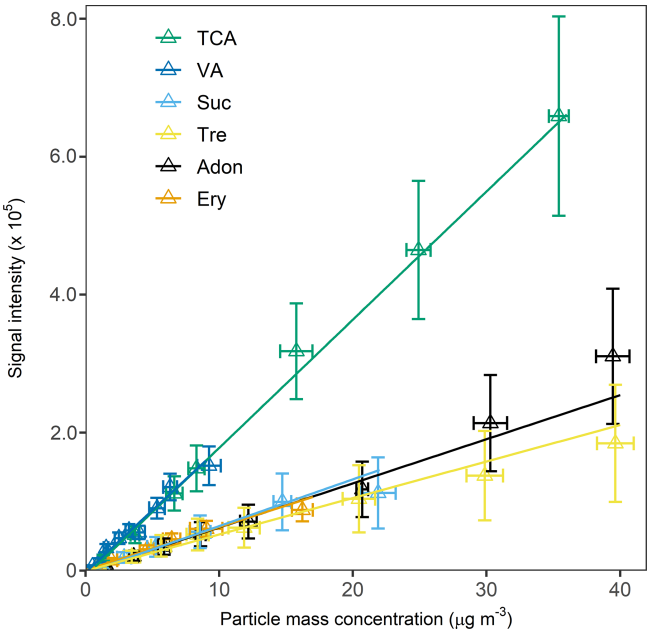

Figure 2. Calibration curves of the six chemical compounds used for sensitivity and LOD determination.

3 Results and discussion

3.1 Characterisation of the HEAC/ESI-Orbitrap-MS system

3.1.1 Sensitivity and LOD

Nebulisation of aqueous solutions of the six chemical standards, namely adonitol, erythritol, sucrose, trehalose, VA and TCA, resulted in aerosol samples with mass concentrations ranging from 0.1 to 30 $\mu g\,m^{-3}$. Calibration curves of the chemical standards are illustrated in Fig. 2. Generally, the ESI-Orbitrap-MS signal intensities of the standards increase linearly with their particle mass concentration. Their sensitivities and LODs are summarised in Table S2. The sensitivities of the standards tested in the present study ranged from $0.53 \pm 0.11 \times 10^4$ (trehalose) to $1.9 \pm 0.21 \times 10^4$ counts $m^3\,\mu g^{-1}$ (TCA). The chemical standards used can be divided into three categories: organic acids (TCA and VA), sugars (sucrose, trehalose), and polyols (adonitol and erythritol). Among these three categories, organic acids have the highest sensitivities. The sensitivities of sugars and polyols fall below 0.7×10^4 counts $m^3\,\mu g^{-1}$. A possible explanation for the above observation is the difference in terms of their ionisation efficiencies under a negative ESI mode (Oss et al., 2010). In general, compounds with a stable anionic form, such as acids, will be efficiently ionised by ESI in the negative-ion mode (Kamel et al., 1999; Ehrmann et al., 2008). The anions of sugars and polyols are less stable, and their ionisation efficiencies are lower than those of organic acids. Therefore, the sensitivities of organic acids are higher than those of sugars and polyols in the present study. The above results show that the functional group of the compound strongly affects its sensitivity in the HEAC/ESI-Orbitrap-MS system.

The chemical standard's LOD was calculated from its sensitivity and background signal's standard deviation, as described in the sensitivity and limit of detection (LOD) calculations section in the Supplement. Among the chemicals tested in the present study, erythritol has the lowest LOD of $1.1 \pm 0.14\,ng\,m^{-3}$. On the other hand, TCA has the highest LOD of $65 \pm 7.4\,ng\,m^{-3}$. The LOD result is of the same order of magnitude as those reported in the literature using similar instrumental techniques. Lopez-Hilfiker et al. (2019) determined the LOD of raffinose and dipentaerythritol of their EESI-TOF instrument to be a few $ng\,m^{-3}$. Zhang et al. (2016) reported the LOD of a wide range of chemical standards, including organic acids and polyols, to be tens of $ng\,m^{-3}$ to a few $\mu g\,m^{-3}$ in their particle-into-liquid sampler (PILS) coupled with a UPLC/ESI-Q-TOFMS system. The slightly lower LOD reported in the present study is probably the result of using Orbitrap-MS as the analyser, which provides a higher mass resolution and, thus, a lower background noise signal than a TOF-MS.

3.1.2 The effect of working fluid on the sensitivity and LOD

To investigate the effect of different solvents as the working fluid in the vortex collector, the sensitivities and LOD of vanillic acid, TCA, and adonitol were determined using Milli-Q water, methanol, and ACN as the working fluids. The results are summarised in Table S3.

In general, the choice of working fluid did not significantly affect the LOD of the chemical compounds as LOD is primarily influenced by the standard deviation of the compound's background signal. However, significant differences in sensitivity were observed among the three working fluids. For the two acids, using ACN as the working fluid resulted in more than twice the sensitivity compared to using methanol or Milli-Q water. For adonitol, Milli-Q water yielded the highest sensitivity, while methanol resulted in the lowest sensitivity for TCA and VA.

Unlike LOD, many factors influence the signal intensity and sensitivity of a compound in ESI-MS, such as the ionisation efficiency during the ESI process, the ionisation energy of the compound in the solvent, and the ion suppression effect caused by other ions in the sample. These factors have mixed effects on the signal intensity and sensitivity of the target compound. Results from this study show no clear pattern for the three working fluids and compounds used. Further research is needed to understand the relationship between the working fluid in the vortex collector and the compound's sensitivity as measured by the ESI-Orbitrap-MS, especially when quantitative analysis is required.

3.1.3 Effects of ESI heater temperature on the signal intensity

To demonstrate the effects of ESI settings on the target compound's signal intensity, the heater temperature of the ESI source was altered while the target compound's concentration introduced into the HEAC/ESI-Orbitrap-MS system was kept constant. The reason for choosing to vary the heater temperature is that it controls the temperature of the auxiliary nitrogen gas, which is used to assist the desolvation of sample solutions. Therefore, it is anticipated that the heater temperature will significantly affect the evaporation of the charged solvent droplet and the ionisation of the target analyte. In this experiment, erythritol was nebulised at a fixed concentration and measured by the HEAC/ESI-Orbitrap-MS system. The ESI heater temperature was increased from 50 to 350 °C with a 50 °C increment. Figure 3 shows the signal intensity of erythritol and the total ion count (TIC, from $m/z = 50$ to 500) in response to the change in heater temperature. It can be observed in the figure that the TIC doubles for every 100 °C increase in heater temperature. This observation agrees with the fact that the rise in heater temperature will enhance the ionisation efficiency of the sample by promoting solvent evaporation in the vaporisation chamber of the ESI source. Similarly, the signal intensity of erythritol increases with heater temperature from 50 to 250 °C. However, when the heater temperature rises above 250 °C, the signal intensity of erythritol starts to drop. This observation likely resulted from the ion suppression effect on the erythritol signal as a result of the high background signal, as reflected by the increase in TIC (Furey et al., 2013). The suppression effect was also observed in background ions (e.g. $m/z = 107$ and 109) unrelated to erythritol. Another possible reason for the decrease in the ion signal of erythritol at a high heater temperature is the thermal decomposition of the compound. Yang et al. (2018) investigated the thermal stability of xylitol and observed its thermal decomposition at around 250 °C. Given the structural similarity between xylitol and erythritol, it is possible that erythritol will undergo thermal decomposition at a similar temperature. However, since there is no reported thermal decomposition temperature of erythritol in the literature, the exact reason for the observed decrease in its signal intensity under high temperatures cannot be concluded in the current study. Nevertheless, the current set of experiments showed that ESI settings, such as heater temperature, will significantly affect the signal intensity of the target compound, and the selection of ESI parameters should be considered during the design of the experiment, especially if quantitative analysis is desired.

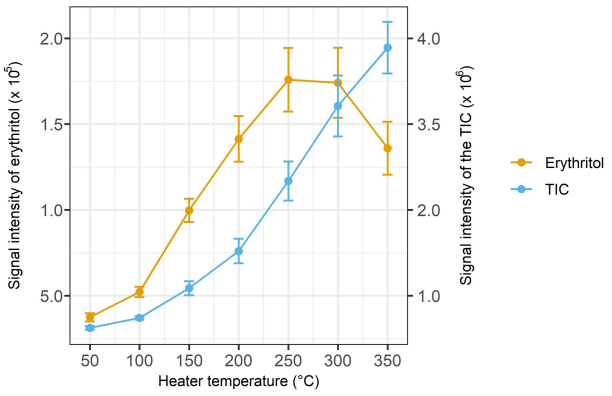

Figure 3. The signal intensity of erythritol and the total ion count (TIC, from $m/z = 50$ to 500) under different heater temperatures.

3.2 α-pinene ozonolysis experiments

3.2.1 Experiment with fast α-pinene injection

Figure 4 shows the mass concentration of particles after injecting 20 µL of α-pinene into the reaction bottle. It can be observed that particles formed almost immediately after the α-pinene injection, and the mass concentration peaked around 5 min after the start of the experiment. After that, the particle mass concentration decreased gradually until reaching the background level. The peak mass concentration was

around 30 $\mu g\,m^{-3}$ in the experiment with fast α-pinene injection.

A typical mass spectrum of the α-pinene ozonolysis products is shown in Fig. 5. Using the product identification workflow described in the methodology section, over 300 ions were assigned as products in the experiment with fast α-pinene injection, including isotope signals of some product ions. Table S4 summarises the product ions observed in the experiment (excluding the isotopes), with a chemical formula predicted from the exact mass of each ion. Figure 6 shows the mass defect plot of α-pinene ozonolysis products identified in the present study. These products cover a wide range of carbon numbers, ranging from 2 to 26 carbon atoms. The bottom-left cluster of products in Fig. 6 corresponds to monomeric compounds with small carbon numbers and low mass defects. Apart from monomeric compounds, dimeric products were observed in the experiment with fast α-pinene ozonolysis, denoted by the upper-right cluster of ions in Fig. 6. This pattern is similar to those observed by Zhang et al. (2017) and Wang et al. (2021), which utilised offline LC/MS techniques for the chemical analysis of the α-pinene ozonolysis products. The similarity between the α-pinene ozonolysis products observed in the current study and those in the literature emphasises the robustness of the HEAC/ESI-Orbitrap-MS in analysing the chemical composition of organic aerosols.

By comparing the exact mass of the product ions with α-pinene ozonolysis products in the literature, some of the ions were assigned chemical structures. These compounds are summarised in Table S5. Figure 4 shows the time series of selected α-pinene ozonolysis products, including cis-pinonic acid, pinalic acid, and 3-methyl-1,2,3-butanetricarboxylic acid (MBTCA). As shown in the figure, the signal intensities of these products follow the particle mass concentration trend measured by the SMPS. Indeed, all of the identified products showed the same signal intensity trend as in Fig. 4. This is probably due to the short reaction time and high initial α-pinene concentration, which suppressed the formation of higher-generation products in the present experiment. Figure S2 shows the hydrogen-to-carbon (H/C) and oxygen-to-carbon (O/C) ratios of the identified products. The figure shows that most products have an O/C ratio smaller than ~ 0.6, indicating a lower degree of oxidation (Molteni et al., 2019). Nevertheless, the agreement between the time profile of the particle's mass concentration and the products' signal intensities confirmed the capability of the HEAC/ESI-Orbitrap-MS system to identify the chemical composition of organic aerosols in real time.

3.2.2 Experiment with slow α-pinene injection

In the experiment with slow α-pinene injection, the evaporation rate of α-pinene was slowed down, and a filter rotation setup was added before the HEAC, as described in the Methodology section. Figure 7 summarises the mass concentration of particles generated from the experiment with slow α-pinene injection. As shown in the figure, a rapid increase in particle mass concentration is observed at the beginning of the first rotation cycle, which marks the start of the α-pinene ozonolysis reaction. In all four rotation cycles, the particle's mass concentration decreases when the HEAC inlet is switched to the charcoal filter and drops to almost zero when changed to the HEPA filter. The rotation between filters sometimes causes a sharp increase in the particle mass concentration because the manual switching of the three-way valve causes pressure fluctuations. The mass concentration of particles decreases during the charcoal filter phase due to the particle loss in the filter. Figure 7 also shows the changes in the signal intensities of selected reaction products measured by the ESI-Orbitrap-MS. It can be observed that the products' signal intensities followed the trend of particle mass concentration. The HEAC/ESI-Orbitrap-MS system's response time, which is the time required for the ESI-Orbitrap-MS signal to reach a steady state after changes in sample concentration, can be estimated from the product's signal intensity time series. As shown in Fig. 7, the increase and decrease in the product's signal intensity take around 2 min to stabilise after each filter change. The response time is mainly governed by the length of the tubing connecting the vortex collector's outlet and the ESI source's inlet. In other words, minimising the length or decreasing the inner diameter of the tubing will shorten the system's response time, which is beneficial in applications involving fast sample composition changes.

A typical mass spectrum of the products in an experiment with slow α-pinene injection during different phases is shown in Fig. S3. The mass spectrum in the no-filter and charcoal filter phases is similar to that obtained from the fast α-pinene injection experiment. This is because, in both experiments, a charcoal filter was connected downstream to the reaction bottle to remove the excess ozone and gas-phase species in the reaction. Samples reaching the HEAC are thus only in the particle phase. This is confirmed by the mass spectrum in the HEPA filter phase, in which the product signals all dropped to background levels.

Another finding in the experiment with slow α-pinene injection is that the HEAC/ESI-Orbitrap-MS can analyse samples with low mass concentration. As outlined in Fig. 7, the mass concentration of α-pinene ozonolysis products decreased over time. During the no-filter phase in the fourth rotation cycle, the mass concentration of particles dropped to below 2 $\mu g\,m^{-3}$. This particle mass concentration is similar to those observed in clean environments. Figure 8 shows the mass spectrum of products during the no-filter phase in the fourth rotation cycle and the time profile of a dimeric reaction product. Despite the low sample concentration, most reaction products are still measurable. The time profile of the dimer showed an increase in signal intensity from 2.29 ± 2.66 in the third HEPA filter phase to 12.15 ± 5.26 in the fourth no-filter phase. This observation emphasised the ability of

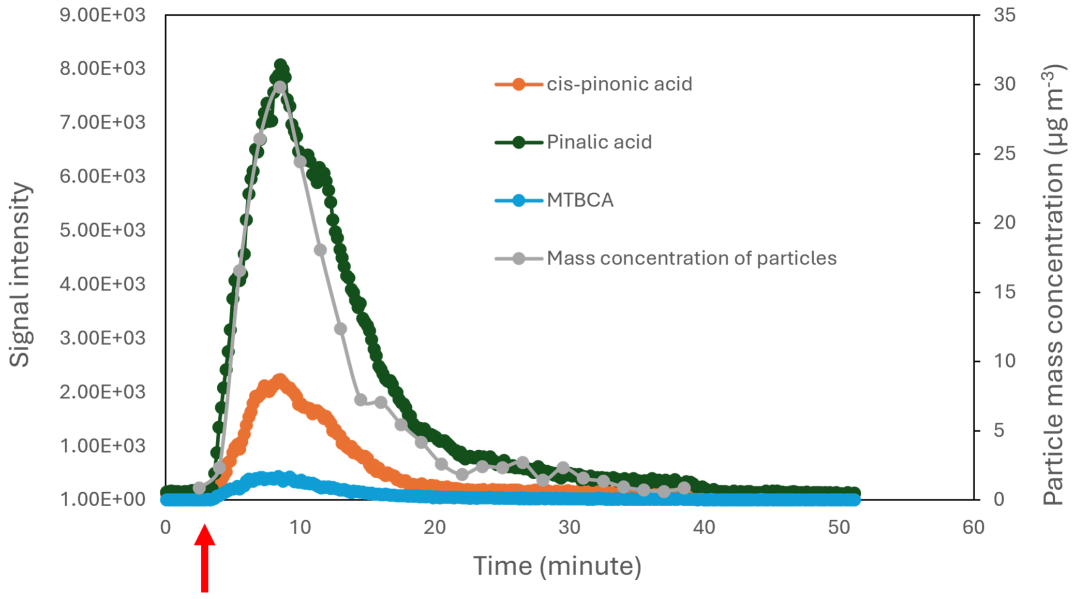

Figure 4. The mass concentration of particles measured by the SMPS and the signal intensity of selected α-pinene ozonolysis products captured by the ESI-Orbitrap-MS for the experiment with fast α-pinene ozonolysis. The red arrow marks the injection time of α-pinene.

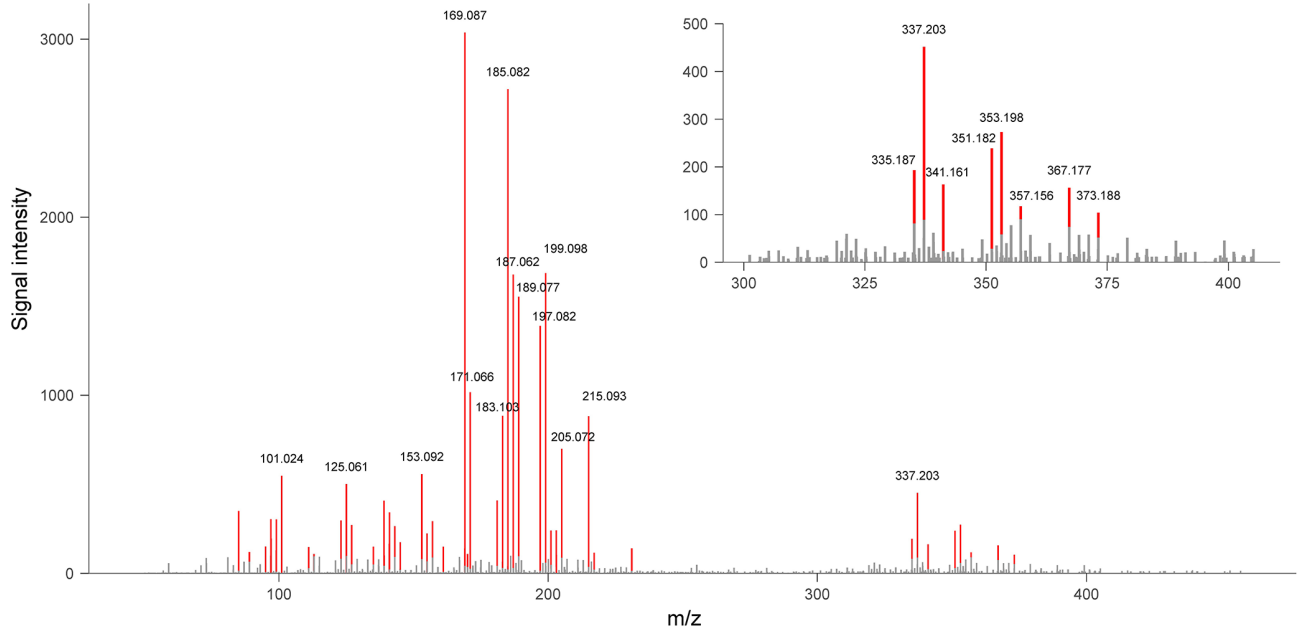

Figure 5. The mass spectrum obtained from the experiment with fast α-pinene injection when the particle mass concentration was the highest. The mass spectrum is background subtracted. Peaks with signal intensity larger than 100 are highlighted in red, and the m/z for peaks with signal intensity larger than 450 are labelled in the figure. The upper-right panel shows the magnification of the $m/z = 300$–400 range of the same mass spectrum. Peaks with signal intensity larger than 100 are highlighted in red and labelled with their corresponding m/z.

the HEAC/ESI-Orbitrap-MS system to analyse the chemical composition of organic aerosols in atmospherically relevant conditions.

4 Limitations and practical considerations

The results of the current study showed that the proposed HEAC/ESI-Orbitrap-MS system has high sensitivities and low LODs in relation to chemical standards and can analyse complex OA samples in real time. Nevertheless, limitations

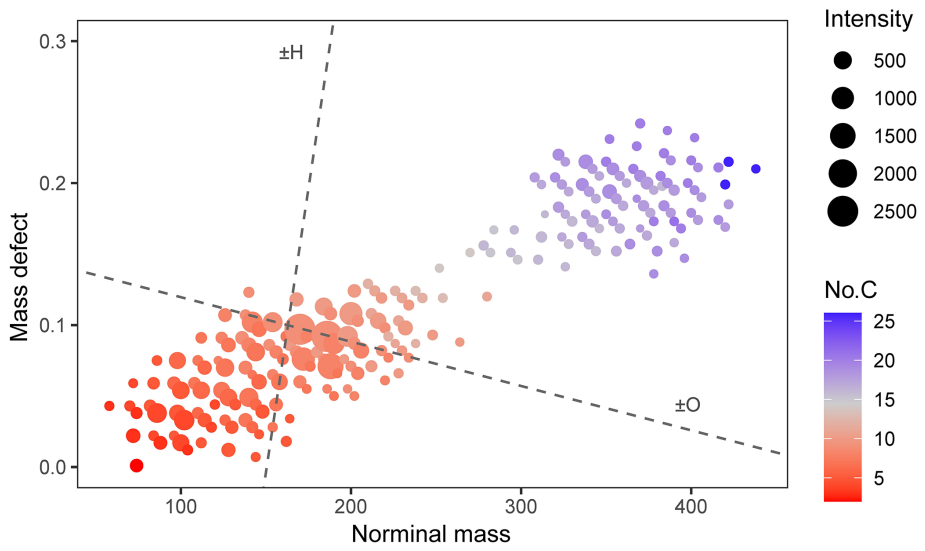

Figure 6. The mass defect plot of the ozonolysis products in the experiment with fast α-pinene injection. The data in the figure correspond to the moment when the particle mass concentration peaked. Dashed lines in the figure represent the changes in mass defect when an oxygen (O) or hydrogen (H) atom was added to a compound. The addition of an H atom will increase the mass defect, while the addition of an O atom will decrease the mass defect of a compound.

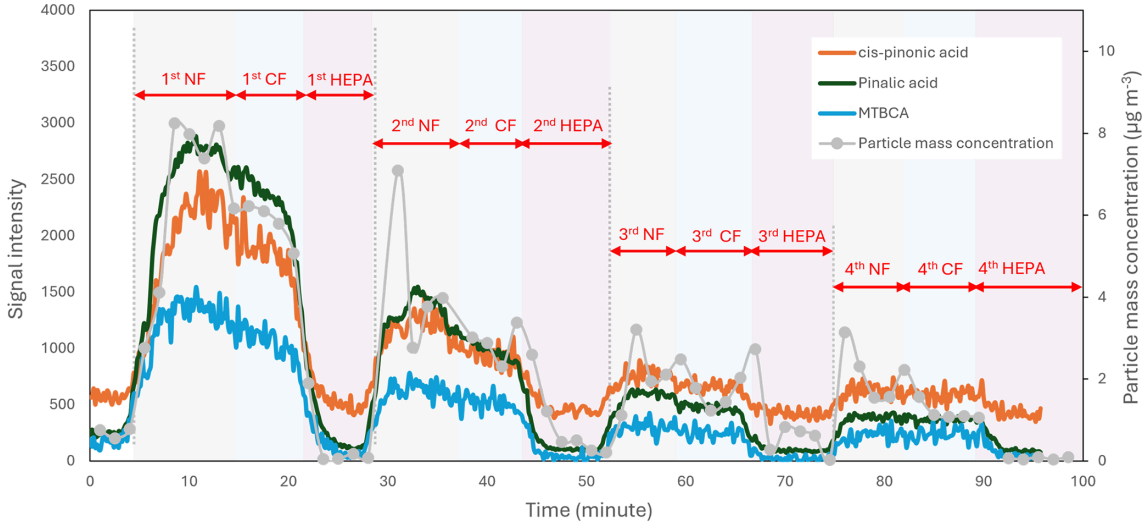

Figure 7. Mass concentration of particles generated from the experiment with slow α-pinene injection and the signal intensity of selected reaction products measured by the ESI-Orbitrap-MS. For each filter rotation cycle, the sample flow went through one of three scenarios before going into HEAC: (1) passing through a HEPA filter (HEPA), (2) passing through a charcoal filter (CF), and (3) passing through no filter (NF).

exist for the HEAC/ESI-Orbitrap-MS system, which will be discussed, together with practical considerations when using the system, in the following sections.

4.1 The choice of working fluid

The HEAC/ESI-Orbitrap-MS system can only identify the chemical composition of the OA fraction soluble in the working fluid because ESI cannot efficiently ionise undissolved compounds. This is a common limitation in all analytical systems utilising ESI to generate sample ions. One trivial way to tackle this problem is to change the working fluid to another solvent in which the target compounds have higher solubility. However, as shown in our results, changing the working fluid will significantly impact the signal intensity and sensitivity of the target compound. Furthermore, although the vortex collector can accommodate most organic solvents, not all are compatible with the ESI-MS. Therefore, it is crucial to identify the compounds of interest during the experimental

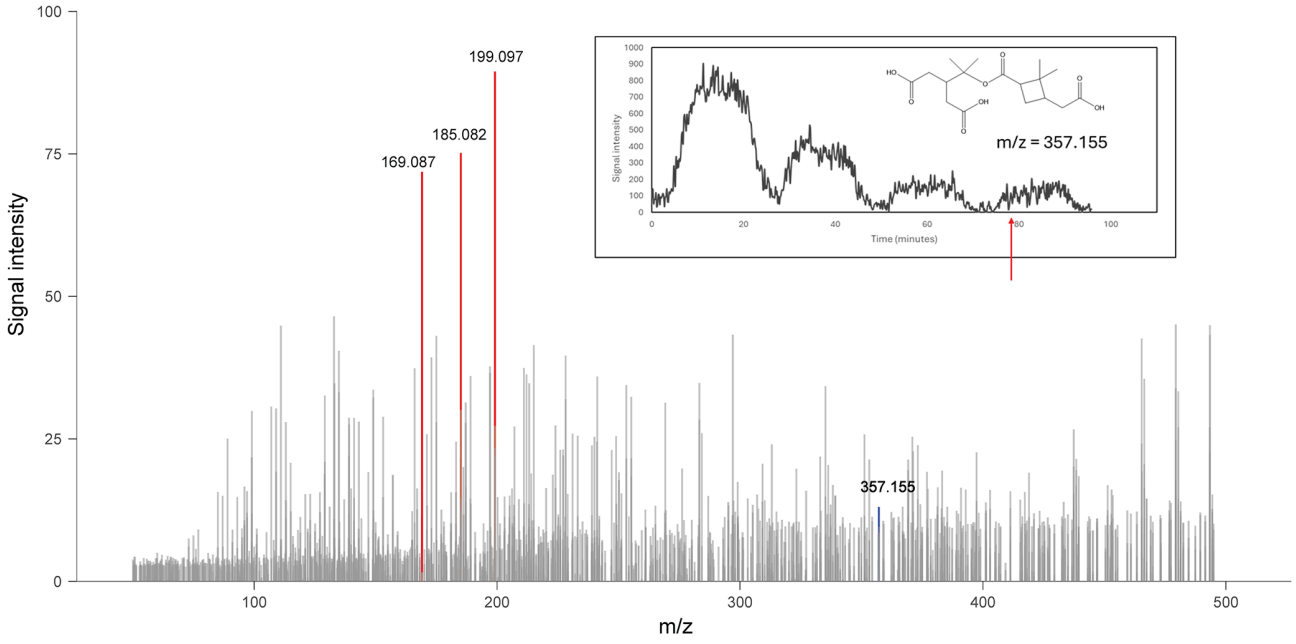

Figure 8. Mass spectrum of products during the no-filter phase in the fourth rotation cycle in the experiment with slow α-pinene injection. Peaks with signal intensities larger than 50 were highlighted in red. The plot embedded in the mass spectrum corresponds to the time profile of a dimeric product with $m/z = 357.155$. The red arrow in the plot corresponds to the time when the mass spectrum is obtained.

planning stage and to consider which solvent to use as the working fluid. If possible, preliminary tests should be done to test the performance of a few different candidates. If there are no specific target compounds, using methanol or ACN as the working fluid is recommended to cover a solubility range that is as wide as possible.

4.2 The response time of the system

Although the HEAC/ESI-Orbitrap-MS is capable of continuous sampling and analysis of OA samples, the time resolution of the instrument depends on the response time of the system, which is the time required for a change in sample composition in front of the HEAC to be reflected by the mass spectrum. As shown in the experiment with slow α-pinene injection, it takes around 2 min for the compound signals to reach a steady state whenever there is a sudden change (e.g. switching the HEAC inlet from no filter to a HEPA filter) in the sample concentration. Therefore, it can be considered to be the case that the compound's signal measured by the MS represents a 2 min average concentration of the compound in the OA sample. This, in turn, means that any changes in sample composition and concentration within the 2 min time frame will not be observable by the MS. Although such rapid changes are rare in atmospheric chemistry, it is desirable to shorten the response time and to increase the time resolution of the system as much as possible. A straightforward way to do this is to shorten the tubing connecting the outlet of the vortex collector and the inlet of the ESI source. Replacing the piston pump in the current setup with a liquid-handling system of smaller internal volume can also minimise the time required for the liquid sample to reach the ESI source.

4.3 Ion suppression and matrix effects of ESI

Ion suppression and matrix effects are well-known issues with ESI sources, hindering their application in accurate quantitative analyses of complex samples like organic aerosols (Parshintsev and Hyötyläinen, 2015). Separation techniques, such as LC and SPE, can be applied before ESI-MS analyses to reduce the influence of ion suppression and matrix effects by reducing the number of co-eluting compounds. However, the additional separation step will reduce the time resolution of the whole system. Since the objective of the present study is to develop a real-time system for the chemical characterisation of organic aerosol with a high time resolution, samples collected by the HEAC were introduced into the ESI source in a direct-infusion manner. Although it is impossible to eliminate the matrix effect when an ESI source is used, some correction can be done and precautionary steps can be taken to minimise or monitor its effects on the target compound's ionisation efficiency. For the proposed HEAC/ESI-Orbitrap-MS system, two practical ways of minimising and monitoring the matrix effect are to minimise the total concentration of compounds in the sample and to add internal standards to the working fluid (Zhou et al., 2017). In particular, the total concentration of analytes should be kept below 10^{-5} M under the current instrumental settings (Furey et al., 2013). This level corresponds to a mass concentration of around 100 $\mu g\,m^{-3}$ of soluble chemical components in the

aerosol sample, assuming an average molecular mass of 200 for the soluble compounds. If the mass loading of the aerosol sample was too high, dilution of the sample should be considered. The sample dilution can be accomplished by diluting the aerosol sample before entry into the HEAC or by infusing a larger amount of solvent into the aqueous sample flow before entry into the ESI source. An internal standard can also be used to monitor the ion suppression effect during the sampling period. Ideally, for targeted analysis, stable-isotope-labelled compounds should be used as they resemble the physical and chemical properties of the target analytes. However, isotope-labelled compounds might not be readily available for the target analytes. Alternatively, compounds with similar chemical functionalities compared to the target analytes that do not exist in the sample can be used as internal standards. The present study added malic acid to the working fluid as an internal standard in experiments with fast and slow α-pinene injection. The malic acid signal did not change in both cases as the α-pinene ozonolysis products reached the MS, as shown in Fig. S4. The above observation showed that ion suppression was minimal under the current experimental conditions and OA mass loading. However, in experiments with high OA mass loadings (e.g. over $200\,\mu g\,m^{-3}$) and using inorganic salts as seed particles, attention must be paid to the ion suppression and matrix effects if doing quantitative data analyses.

4.4 Other considerations in experimental designs

As described by Brown et al. (2019b), the HEAC collects samples into the working fluid regardless of their solubility. A highly insoluble material content in the sample flow might block the ESI nozzle and decrease the spray's performance. In experiments anticipated to have a high emission rate of insoluble particles, such as biomass burning simulations, in-line filters should be used to remove the insoluble particles before the ESI source. Besides this, the current prototype HEAC/ESI-Orbitrap-MS setup utilised a single-piston pump for the sample injection. Although able to achieve continuous sample injection, the single-piston pump also introduced significant pulsations into the sample flow. Replacing the pump with a double-piston pump or another liquid-handling system with minimal pulsation can potentially increase the performance of the system and the readability of the mass spectrum.

5 Conclusion

The current study introduces an innovative system for the real-time chemical characterisation of organic aerosol particles. The system combines a HEAC for sample collection with an ESI-Orbitrap-MS for chemical analysis. The synergy of these instruments enables continuous sampling and real-time chemical analysis. Results demonstrate that the HEAC/ESI-Orbitrap-MS system offers comparable or even better sensitivity and LOD compared to similar techniques. α-pinene ozonolysis experiments further confirm the system's ability to provide real-time chemical insights into a complex organic aerosol sample. With its soft ionisation source, the system identifies intact chemical compounds, minimising molecular fragmentation. The Orbitrap-MS delivers high-mass-resolution spectra, facilitating precise product identification and isobaric ion separation. Even under low OA mass concentrations ($< 2\,\mu g\,m^{-3}$), the system accurately identifies OA composition, highlighting its ability to chemically characterise OA at atmospherically relevant mass loadings.

Code availability. Only third-party software was used for the data processing and analysis of the current study (R Development Core Team, 2023; Schmid et al., 2023; He et al., 2015). All functions and packages in the software were built in or developed by other studies (Smith et al., 2006; Vermeesch, 2018; Wickham, 2016; York et al., 2004). No code or packages were created in the current study.

Data availability. The authors confirm that the data supporting the findings of this study are available within the article and its Supplement. Raw data are available from the authors on request.

Supplement. The supplement related to this article is available online at https://doi.org/10.5194/amt-18-3945-2025-supplement.

Author contributions. YSL and BM designed the experiment. YSL carried out the experiment, analysed the data, and wrote the paper. BM and ZR supervised and provided comments on the experimental work. All of the authors reviewed and provided feedback on the paper.

Competing interests. The contact author has declared that none of the authors has any competing interests.

Disclaimer. Publisher's note: Copernicus Publications remains neutral with regard to jurisdictional claims made in the text, published maps, institutional affiliations, or any other geographical representation in this paper. While Copernicus Publications makes every effort to include appropriate place names, the final responsibility lies with the authors.

Acknowledgements. This work was enabled by the use of the Central Analytical Research Facility (CARF) at the Queensland University of Technology (QUT). The authors thank David Marshall from CARF for his assistance with the ESI-Orbitrap-MS setup and data analysis.

Review statement. This paper was edited by Charles Brock and reviewed by two anonymous referees.

References

Bates, J. T., Fang, T., Verma, V., Zeng, L., Weber, R. J., Tolbert, P. E., Abrams, J. Y., Sarnat, S. E., Klein, M., Mulholland, J. A., and Russell, A. G.: Review of acellular assays of ambient particulate matter oxidative potential: methods and relationships with composition, sources, and health effects, Environ. Sci. Technol., 53, 4003–4019, https://doi.org/10.1021/acs.est.8b03430, 2019.

Brown, R., Stevanovic, S., Brown, Z., Cai, M., Zhou, S., Song, W., Wang, X., Miljevic, B., Zhao, J., Bottle, S., and Ristovski, Z.: Application of a fluorescent probe for the online Measurement of PM-bound reactive oxygen species in chamber and ambient studies, Sensors, 19, 4564, https://doi.org/10.3390/s19204564, 2019a.

Brown, R. A., Stevanovic, S., Bottle, S., and Ristovski, Z. D.: An instrument for the rapid quantification of PM-bound ROS: the Particle Into Nitroxide Quencher (PINQ), Atmos. Meas. Tech., 12, 2387–2401, https://doi.org/10.5194/amt-12-2387-2019, 2019b.

Brown, R. A., Stevanovic, S., Bottle, S., Wang, H., Hu, Z., Wu, C., Wang, B., and Ristovski, Z.: Relationship between atmospheric PM-bound reactive oxygen species, their half-lives, and regulated pollutants: investigation and preliminary model, Environ. Sci. Technol., 54, 4995–5002, https://doi.org/10.1021/acs.est.9b06643, 2020.

Budisulistiorini, S. H., Li, X., Bairai, S. T., Renfro, J., Liu, Y., Liu, Y. J., McKinney, K. A., Martin, S. T., McNeill, V. F., Pye, H. O. T., Nenes, A., Neff, M. E., Stone, E. A., Mueller, S., Knote, C., Shaw, S. L., Zhang, Z., Gold, A., and Surratt, J. D.: Examining the effects of anthropogenic emissions on isoprene-derived secondary organic aerosol formation during the 2013 Southern Oxidant and Aerosol Study (SOAS) at the Look Rock, Tennessee ground site, Atmos. Chem. Phys., 15, 8871–8888, https://doi.org/10.5194/acp-15-8871-2015, 2015.

Canagaratna, M. R., Jayne, J. T., Jimenez, J. L., Allan, J. D., Alfarra, M. R., Zhang, Q., Onasch, T. B., Drewnick, F., Coe, H., Middlebrook, A., Delia, A., Williams, L. R., Trimborn, A. M., Northway, M. J., DeCarlo, P. F., Kolb, C. E., Davidovits, P., and Worsnop, D. R.: Chemical and microphysical characterization of ambient aerosols with the aerodyne aerosol mass spectrometer, Mass Spectrom. Rev., 26, 185–222, https://doi.org/10.1002/mas.20115, 2007.

Ehrmann, B. M., Henriksen, T., and Cech, N. B.: Relative importance of basicity in the gas phase and in solution for determining selectivity in electrospray ionization mass spectrometry, J. Am. Soc. Mass Spectr., 19, 719–728, https://doi.org/10.1016/j.jasms.2008.01.003, 2008.

Fan, J., Wang, Y., Rosenfeld, D., and Liu, X.: Review of aerosol–cloud interactions: mechanisms, significance, and challenges, J. Atmos. Sci., 73, 4221–4252, https://doi.org/10.1175/JAS-D-16-0037.1, 2016.

Fleming, L. T., Lin, P., Roberts, J. M., Selimovic, V., Yokelson, R., Laskin, J., Laskin, A., and Nizkorodov, S. A.: Molecular composition and photochemical lifetimes of brown carbon chromophores in biomass burning organic aerosol, Atmos. Chem. Phys., 20, 1105–1129, https://doi.org/10.5194/acp-20-1105-2020, 2020.

Furey, A., Moriarty, M., Bane, V., Kinsella, B., and Lehane, M.: Ion suppression; A critical review on causes, evaluation, prevention and applications, Talanta, 115, 104–122, https://doi.org/10.1016/j.talanta.2013.03.048, 2013.

He, L., Diedrich, J., Chu, Y.-Y., and Yates III, J. R.: Extracting accurate precursor information for tandem mass spectra by RawConverter, Anal. Chem., 87, 11361–11367, https://doi.org/10.1021/acs.analchem.5b02721, 2015.

Huang, R.-J., Zhang, Y., Bozzetti, C., Ho, K.-F., Cao, J.-J., Han, Y., Daellenbach, K. R., Slowik, J. G., Platt, S. M., Canonaco, F., Zotter, P., Wolf, R., Pieber, S. M., Bruns, E. A., Crippa, M., Ciarelli, G., Piazzalunga, A., Schwikowski, M., Abbaszade, G., Schnelle-Kreis, J., Zimmermann, R., An, Z., Szidat, S., Baltensperger, U., Haddad, I. E., and Prévôt, A. S. H.: High secondary aerosol contribution to particulate pollution during haze events in China, Nature, 514, 218–222, https://doi.org/10.1038/nature13774, 2014.

Jimenez, J. L., Canagaratna, M. R., Donahue, N. M., Prevot, A. S. H., Zhang, Q., Kroll, J. H., DeCarlo, P. F., Allan, J. D., Coe, H., Ng, N. L., Aiken, A. C., Docherty, K. S., Ulbrich, I. M., Grieshop, A. P., Robinson, A. L., Duplissy, J., Smith, J. D., Wilson, K. R., Lanz, V. A., Hueglin, C., Sun, Y. L., Tian, J., Laaksonen, A., Raatikainen, T., Rautiainen, J., Vaattovaara, P., Ehn, M., Kulmala, M., Tomlinson, J. M., Collins, D. R., Cubison, M. J., Dunlea, J., Huffman, J. A., Onasch, T. B., Alfarra, M. R., Williams, P. I., Bower, K., Kondo, Y., Schneider, J., Drewnick, F., Borrmann, S., Weimer, S., Demerjian, K., Salcedo, D., Cottrell, L., Griffin, R., Takami, A., Miyoshi, T., Hatakeyama, S., Shimono, A., Sun, J. Y., Zhang, Y. M., Dzepina, K., Kimmel, J. R., Sueper, D., Jayne, J. T., Herndon, S. C., Trimborn, A. M., Williams, L. R., Wood, E. C., Middlebrook, A. M., Kolb, C. E., Baltensperger, U., and Worsnop, D. R.: Evolution of organic aerosols in the atmosphere, Science, 326, 1525, https://doi.org/10.1126/science.1180353, 2009.

Kamel, A. M., Brown, P. R., and Munson, B.: Effects of mobile-phase additives, solution pH, ionization constant, and analyte concentration on the sensitivities and electrospray ionization mass spectra of nucleoside antiviral agents, Anal. Chem., 71, 5481–5492, https://doi.org/10.1021/ac9906429, 1999.

Kanakidou, M., Seinfeld, J. H., Pandis, S. N., Barnes, I., Dentener, F. J., Facchini, M. C., Van Dingenen, R., Ervens, B., Nenes, A., Nielsen, C. J., Swietlicki, E., Putaud, J. P., Balkanski, Y., Fuzzi, S., Horth, J., Moortgat, G. K., Winterhalter, R., Myhre, C. E. L., Tsigaridis, K., Vignati, E., Stephanou, E. G., and Wilson, J.: Organic aerosol and global climate modelling: a review, Atmos. Chem. Phys., 5, 1053–1123, https://doi.org/10.5194/acp-5-1053-2005, 2005.

Kautzman, K. E., Surratt, J. D., Chan, M. N., Chan, A. W. H., Hersey, S. P., Chhabra, P. S., Dalleska, N. F., Wennberg, P. O., Flagan, R. C., and Seinfeld, J. H.: Chemical composition of gas- and aerosol-phase products from the photooxidation of naphthalene, J. Phys. Chem. A, 114, 913–934, https://doi.org/10.1021/jp908530s, 2010.

Kirchstetter, T. W., Corrigan, C. E., and Novakov, T.: Laboratory and field investigation of the adsorption of gaseous organic compounds onto quartz filters, Atmos. Environ., 35, 1663–1671, https://doi.org/10.1016/S1352-2310(00)00448-9, 2001.

Krechmer, J. E., Groessl, M., Zhang, X., Junninen, H., Massoli, P., Lambe, A. T., Kimmel, J. R., Cubison, M. J., Graf, S., Lin, Y.-H., Budisulistiorini, S. H., Zhang, H., Surratt, J. D., Knochenmuss, R., Jayne, J. T., Worsnop, D. R., Jimenez, J.-L., and Canagaratna, M. R.: Ion mobility spectrometry–mass spectrometry (IMS–MS) for on- and offline analysis of atmospheric gas and aerosol species, Atmos. Meas. Tech., 9, 3245–3262, https://doi.org/10.5194/amt-9-3245-2016, 2016.

Kulkarni, P., Baron, P. A., and Willeke, K.: Aerosol measurement: principles, techniques, and applications, 3rd edn., John Wiley and Sons, Incorporated, https://doi.org/10.1002/9781118001684, 2011.

Kwon, H.-S., Ryu, M. H., and Carlsten, C.: Ultrafine particles: unique physicochemical properties relevant to health and disease, Exp. Mol. Med., 52, 318–328, https://doi.org/10.1038/s12276-020-0405-1, 2020.

Lopez-Hilfiker, F. D., Pospisilova, V., Huang, W., Kalberer, M., Mohr, C., Stefenelli, G., Thornton, J. A., Baltensperger, U., Prevot, A. S. H., and Slowik, J. G.: An extractive electrospray ionization time-of-flight mass spectrometer (EESI-TOF) for online measurement of atmospheric aerosol particles, Atmos. Meas. Tech., 12, 4867–4886, https://doi.org/10.5194/amt-12-4867-2019, 2019.

Mahowald, N., Ward, D. S., Kloster, S., Flanner, M. G., Heald, C. L., Heavens, N. G., Hess, P. G., Lamarque, J.-F., and Chuang, P. Y.: Aerosol impacts on climate and biogeochemistry, Annu. Rev. Env. Resour., 36, 45–74, https://doi.org/10.1146/annurev-environ-042009-094507, 2011.

McNeill, V. F.: Atmospheric aerosols: clouds, chemistry, and climate, Annu. Rev. Chem. Biomol., 8, 427–444, https://doi.org/10.1146/annurev-chembioeng-060816-101538, 2017.

Miljevic, B., Hedayat, F., Stevanovic, S., Fairfull-Smith, K. E., Bottle, S. E., and Ristovski, Z. D.: To sonicate or not to Sonicate PM filters: reactive oxygen species generation upon ultrasonic irradiation, Aerosol Sci. Tech., 48, 1276–1284, https://doi.org/10.1080/02786826.2014.981330, 2014.

Molteni, U., Simon, M., Heinritzi, M., Hoyle, C. R., Bernhammer, A.-K., Bianchi, F., Breitenlechner, M., Brilke, S., Dias, A., Duplissy, J., Frege, C., Gordon, H., Heyn, C., Jokinen, T., Kürten, A., Lehtipalo, K., Makhmutov, V., Petäjä, T., Pieber, S. M., Praplan, A. P., Schobesberger, S., Steiner, G., Stozhkov, Y., Tomé, A., Tröstl, J., Wagner, A. C., Wagner, R., Williamson, C., Yan, C., Baltensperger, U., Curtius, J., Donahue, N. M., Hansel, A., Kirkby, J., Kulmala, M., Worsnop, D. R., and Dommen, J.: Formation of highly oxygenated organic molecules from α-pinene ozonolysis: chemical characteristics, mechanism, and kinetic model development, ACS Earth Space Chem., 3, 873–883, https://doi.org/10.1021/acsearthspacechem.9b00035, 2019.

Myers, O. D., Sumner, S. J., Li, S., Barnes, S., and Du, X.: One step forward for reducing false positive and false negative compound identifications from mass spectrometry metabolomics data: new algorithms for constructing extracted ion chromatograms and detecting chromatographic peaks, Anal. Chem., 89, 8696–8703, https://doi.org/10.1021/acs.analchem.7b00947, 2017.

Orsini, D. A., Rhoads, K., McElhoney, K., Schick, E., Koehler, D., and Hogrefe, O.: A water cyclone to preserve insoluble aerosols in liquid flow – an interface to flow cytometry to detect airborne nucleic acid, Aerosol Sci. Tech., 42, 343–356, https://doi.org/10.1080/02786820802072881, 2008.

Oss, M., Kruve, A., Herodes, K., and Leito, I.: Electrospray ionization efficiency scale of organic compounds, Anal. Chem., 82, 2865–2872, https://doi.org/10.1021/ac902856t, 2010.

Parshintsev, J. and Hyötyläinen, T.: Methods for characterization of organic compounds in atmospheric aerosol particles, Anal. Bioanal. Chem., 407, 5877–5897, https://doi.org/10.1007/s00216-014-8394-3, 2015.

Parshintsev, J., Kivilompolo, M., Ruiz-Jimenez, J., Hartonen, K., Kulmala, M., and Riekkola, M.-L.: Particle-into-liquid sampler on-line coupled with solid-phase extraction-liquid chromatography–mass spectrometry for the determination of organic acids in atmospheric aerosols, J. Chromatogr. A, 1217, 5427–5433, https://doi.org/10.1016/j.chroma.2010.06.026, 2010.

Piel, F., Müller, M., Mikoviny, T., Pusede, S. E., and Wisthaler, A.: Airborne measurements of particulate organic matter by proton-transfer-reaction mass spectrometry (PTR-MS): a pilot study, Atmos. Meas. Tech., 12, 5947–5958, https://doi.org/10.5194/amt-12-5947-2019, 2019.

Pluskal, T., Castillo, S., Villar-Briones, A., and Orešič, M.: MZmine 2: Modular framework for processing, visualizing, and analyzing mass spectrometry-based molecular profile data, BMC Bioinformatics, 11, 395, https://doi.org/10.1186/1471-2105-11-395, 2010.

Pöschl, U.: Atmospheric aerosols: composition, transformation, climate and health effects, Angew. Chem. Int. Edit., 44, 7520–7540, https://doi.org/10.1002/anie.200501122, 2005.

R Development Core Team: R: A language and environment for statistical computing, R foundation for statistical computing [code], https://www.R-project.org/ (last access: 19 August 2025), 2023.

Quinn, P. K., Collins, D. B., Grassian, V. H., Prather, K. A., and Bates, T. S.: Chemistry and related properties of freshly emitted sea spray aerosol, Chem. Rev., 115, 4383–4399, https://doi.org/10.1021/cr500713g, 2015.

Saarnio, K., Teinilä, K., Saarikoski, S., Carbone, S., Gilardoni, S., Timonen, H., Aurela, M., and Hillamo, R.: Online determination of levoglucosan in ambient aerosols with particle-into-liquid sampler–high-performance anion-exchange chromatography–mass spectrometry (PILS–HPAEC–MS), Atmos. Meas. Tech., 6, 2839–2849, https://doi.org/10.5194/amt-6-2839-2013, 2013.

Schmid, R., Heuckeroth, S., Korf, A., Smirnov, A., Myers, O., Dyrlund, T. S., Bushuiev, R., Murray, K. J., Hoffmann, N., Lu, M., Sarvepalli, A., Zhang, Z., Fleischauer, M., Dührkop, K., Wesner, M., Hoogstra, S. J., Rudt, E., Mokshyna, O., Brungs, C., Ponomarov, K., Mutabdžija, L., Damiani, T., Pudney, C. J., Earll, M., Helmer, P. O., Fallon, T. R., Schulze, T., Rivas-Ubach, A., Bilbao, A., Richter, H., Nothias, L.-F., Wang, M., Orešič, M., Weng, J.-K., Böcker, S., Jeibmann, A., Hayen, H., Karst, U., Dorrestein, P. C., Petras, D., Du, X., and Pluskal, T.: Integrative analysis of multimodal mass spectrometry data in MZmine 3, Nat. Biotechnol., 41, 447–449, https://doi.org/10.1038/s41587-023-01690-2, 2023.

Shilling, J. E., Chen, Q., King, S. M., Rosenoern, T., Kroll, J. H., Worsnop, D. R., DeCarlo, P. F., Aiken, A. C., Sueper, D., Jimenez, J. L., and Martin, S. T.: Loading-dependent elemental

composition of α-pinene SOA particles, Atmos. Chem. Phys., 9, 771–782, https://doi.org/10.5194/acp-9-771-2009, 2009.

Shiraiwa, M., Ueda, K., Pozzer, A., Lammel, G., Kampf, C. J., Fushimi, A., Enami, S., Arangio, A. M., Fröhlich-Nowoisky, J., Fujitani, Y., Furuyama, A., Lakey, P. S. J., Lelieveld, J., Lucas, K., Morino, Y., Pöschl, U., Takahama, S., Takami, A., Tong, H., Weber, B., Yoshino, A., and Sato, K.: Aerosol health effects from molecular to global scales, Environ. Sci. Technol., 51, 13545–13567, https://doi.org/10.1021/acs.est.7b04417, 2017.

Shrivastava, M., Cappa, C. D., Fan, J., Goldstein, A. H., Guenther, A. B., Jimenez, J. L., Kuang, C., Laskin, A., Martin, S. T., Ng, N. L., Petaja, T., Pierce, J. R., Rasch, P. J., Roldin, P., Seinfeld, J. H., Shilling, J., Smith, J. N., Thornton, J. A., Volkamer, R., Wang, J., Worsnop, D. R., Zaveri, R. A., Zelenyuk, A., and Zhang, Q.: Recent advances in understanding secondary organic aerosol: Implications for global climate forcing, Rev. Geophys., 55, 509–559, https://doi.org/10.1002/2016rg000540, 2017.

Smith, C. A., Want, E. J., O'Maille, G., Abagyan, R., and Siuzdak, G.: XCMS: Processing Mass Spectrometry Data for Metabolite Profiling Using Nonlinear Peak Alignment, Matching, and Identification, Anal. Chem., 78, 779–787, https://doi.org/10.1021/ac051437y, 2006.

Stockwell, C. E., Kupc, A., Witkowski, B., Talukdar, R. K., Liu, Y., Selimovic, V., Zarzana, K. J., Sekimoto, K., Warneke, C., Washenfelder, R. A., Yokelson, R. J., Middlebrook, A. M., and Roberts, J. M.: Characterization of a catalyst-based conversion technique to measure total particulate nitrogen and organic carbon and comparison to a particle mass measurement instrument, Atmos. Meas. Tech., 11, 2749–2768, https://doi.org/10.5194/amt-11-2749-2018, 2018.

Sun, Y., Du, W., Fu, P., Wang, Q., Li, J., Ge, X., Zhang, Q., Zhu, C., Ren, L., Xu, W., Zhao, J., Han, T., Worsnop, D. R., and Wang, Z.: Primary and secondary aerosols in Beijing in winter: sources, variations and processes, Atmos. Chem. Phys., 16, 8309–8329, https://doi.org/10.5194/acp-16-8309-2016, 2016.

Tao, J., Zhang, L., Cao, J., and Zhang, R.: A review of current knowledge concerning $PM_{2.5}$ chemical composition, aerosol optical properties and their relationships across China, Atmos. Chem. Phys., 17, 9485–9518, https://doi.org/10.5194/acp-17-9485-2017, 2017.

Vermeesch, P.: IsoplotR: A free and open toolbox for geochronology, Geosci. Front., 9, 1479–1493, https://doi.org/10.1016/j.gsf.2018.04.001, 2018.

Wang, Y., Zhao, Y., Li, Z., Li, C., Yan, N., and Xiao, H.: Importance of hydroxyl radical chemistry in isoprene suppression of particle formation from α-pinene ozonolysis, ACS Earth Space Chem., 5, 487–499, https://doi.org/10.1021/acsearthspacechem.0c00294, 2021.

Wickham, H.: Data Analysis, in: ggplot2: Elegant Graphics for Data Analysis, edited by: Wickham, H., Springer International Publishing, Cham, 189–201, https://doi.org/10.1007/978-3-319-24277-4_9, 2016.

Yang, Y., Kong, W., and Cai, X.: Solvent-free preparation and performance of novel xylitol based solid-solid phase change materials for thermal energy storage, Energ. Buildings, 158, 37–42, https://doi.org/10.1016/j.enbuild.2017.09.096, 2018.

York, D., Evensen, N. M., Martı´nez, M. L., and De Basabe Delgado, J.: Unified equations for the slope, intercept, and standard errors of the best straight line, Am. J. Phys., 72, 367–375, https://doi.org/10.1119/1.1632486, 2004.

Zhang, X., Dalleska, N. F., Huang, D. D., Bates, K. H., Sorooshian, A., Flagan, R. C., and Seinfeld, J. H.: Time-resolved molecular characterization of organic aerosols by PILS + UPLC/ESI-Q-TOFMS, Atmos. Environ., 130, 180–189, https://doi.org/10.1016/j.atmosenv.2015.08.049, 2016.

Zhang, X., Lambe, A. T., Upshur, M. A., Brooks, W. A., Gray Bé, A., Thomson, R. J., Geiger, F. M., Surratt, J. D., Zhang, Z., Gold, A., Graf, S., Cubison, M. J., Groessl, M., Jayne, J. T., Worsnop, D. R., and Canagaratna, M. R.: Highly oxygenated multifunctional compounds in α-pinene secondary organic aerosol, Environ. Sci. Technol., 51, 5932–5940, https://doi.org/10.1021/acs.est.6b06588, 2017.

Zhou, W., Shuang, Y., and and Wang, P. G.: Matrix effects and application of matrix effect factor, Bioanalysis, 9, 1839–1844, https://doi.org/10.4155/bio-2017-0214, 2017.

Zubarev, R. A. and Makarov, A.: Orbitrap mass spectrometry, Anal. Chem., 85, 5288–5296, https://doi.org/10.1021/ac4001223, 2013.